

Supplementary Information

Mesoporous graphitic carbon nitride@NiCo₂O₄ nanocomposite as solid phase microextraction coating for sensitive determination of environmental pollutants in human serum sample

Jing Zhang,^a Wenqi Li,^a Wenli Zhu,^a Peige Qin,^a Minghua Lu^{*a}, Xuebin Zhang,^b Yuchen Miao,^b and Zongwei Cai^{*c}

^a Henan International Joint Laboratory of Medicinal Plants Utilization, School of Chemistry and Chemical Engineering, Henan University, Kaifeng 475004, Henan, China. E-mail: mhlu@henu.edu.cn

^b Center for Multi-Omics Research, State Key Laboratory of Cotton Biology, Institute of Plant Stress Biology, Henan University, Kaifeng 475004, Henan, China

^c State Key Laboratory of Environmental and Biological Analysis, Department of Chemistry, Hong Kong Baptist University, Hong Kong SAR, China. E-mail: zwcai@hkbu.edu.hk

1. Experiments

1.1 Reagents and materials

Ni(NO₃)₂·6H₂O, Co(NO₃)₂·6H₂O, tetraethyl silicate (TEOS, C₂H₅O₄Si), ammonium bifluoride (NH₄HF₂), hexamethylenetetramine (HMTA, C₆H₁₂N₄), PCBs containing 4-Chlorobiphenyl (PCB-3), 3,4-Dichlorobiphenyl (PCB-12) and 3,5-Dichlorobiphenyl (PCB-14), PAHs including naphthalene (NAP), acenaphthene (ANE), fluorene (FLU), phenanthrene (PHE), anthracene (ANT) and pyrene (PYR) were acquired from Aladdin (Shanghai, China). P123 (Mw=5800, PEO₂₀PPO₇₀PEO₂₀), poly (diallyldimethylammonium chloride) solution (PDDA) were purchased from Sigma-Aldrich (St. Louis, MO, USA). HPLC grade acetone (ACE) were obtained from Merck KGaA (Darmstadt, Germany). Dehydrated alcohol (EtOH), hydrochloric acid (HCl), nitric acid (HNO₃) and urea were received from Kermel chemical reagent Co., Ltd. (Tianjin, China). Ultrapure water (18.2 MΩ cm⁻¹) purified with a Milli-Q purification system (Millipore, Bedford, MA, USA) was used throughout the experiments. All the chemicals were of analytical grade.

Single stock standard solutions of three PCBs and six PAHs were prepared in ACE at a concentration of 0.1 mg·mL⁻¹. The mixed stock standard solution was obtained by diluting each single stock solution with ACE stepwise. The working standard solutions were prepared by a suitable dilution of the mixed stock standard solution with ultrapure water. Above mentioned standard solution were stored at 4 °C in the darkness.

1.2 Instruments

All chromatographic analysis were performed on an Agilent 7890B gas chromatography equipped with a HP-5 capillary column (30 m×0.32 mm×0.25 μm) and a flame ionization detector (FID). High purity nitrogen (99.99%) was used as carrier gas at a constant flow rate of 1.0 mL·min⁻¹. The injector temperature was set at 290 °C and fiber desorption was carried out for 2.5 min under the splitless mode. The detector temperature was 300 °C. The GC oven temperature program was set as

follows: initially maintained at 60 °C for 1 min, then increased to 190 °C (held for 1 min) with a rate of 65 °C·min⁻¹, and again ramped at 6 °C·min⁻¹ to 220 °C held for 0.5 min, finally heated to 300 °C at a rate of 80 °C·min⁻¹ and held for 1 min, the total running time was 11.5 min.

The structure and morphology of the fiber coating was characterized by using a ZEISS GeminiSEM 500 (England) scanning electron microscopy (SEM) assembled with energy dispersive X-ray spectrometer (EDS). The X-ray powder diffraction (XRD) measurement was recorded on a Bruker D8 Advance X-ray diffractometer with Cu K α radiation. Infrared absorption spectrum was performed on an infrared Fourier transform spectrometer (Bruker, VERTEX 70). Thermogravimetric analysis experiments (TGA, QMS 403 D Aëolos®, NETZSCH, Germany) was performed to evaluate the thermal stability of the fiber coating from room temperature to 800 °C in flowing N₂ at heating rate of 10 °C·min⁻¹.

1.3 Preparation SPME coating

1.3.1 Synthesis of MCN

The synthesis of MCN was according to our previous described methods by using a green hexamethylenetetramine as precursor and SBA-15 as silica template.¹ Initially, 1.0 g of SBA-15 template was dispersed in the mixture solution of 10.0 mL ultrapure water and 8.0 g HMTA with straight stirring for 5 h at the room temperature. Subsequently, the mixture was evaporated at 50 °C to remove water. The obtained white solid was dried in an oven overnight, followed by heated to 550 °C in nitrogen atmosphere for 4 h with the ramping rate of 2 °C·min⁻¹. Then, the result dark powder was treated with 4 M NH₄HF₂ aqueous solution for 48 h to remove silica framework. Lastly, the dark sample was collected by centrifugation, washed with ultrapure water and ethanol several times and dried under vacuum for 4 h at 60 °C. The required mesoporous graphitic carbon nitride samples were labeled as MCN for convenience.

1.3.2 Synthesis of MCN@NiCo₂O₄ composites

The NiCo₂O₄@MCN nanocomposites were synthesized via a hydrothermal method. Initially, the as-prepared MCN (100 mg) was dispersed into 40 mL deionized water under sonication. Afterwards, 1 mmol Ni(NO₃)₂·6H₂O, 2 mmol Co(NO₃)₂·6H₂O, 5 mmol urea and 4 mL PDDA were further added. After strongly stirring for 1 h, the above solution was transferred into Teflon-lined stainless steel autoclave and heated to 120 °C for 12 h. Then, the precipitates were collected through centrifugation, washed thoroughly with deionized water and ethanol several times, and dried at 80 °C overnight. Finally, the as-grown precursors were annealing at 350 °C for 2 h with a temperature ramp rate of 1 °C·min⁻¹. By changing added amount of NiCo₂O₄ (0.5 mmol, 1 mmol and 2 mmol), MCN@NiCo₂O₄ composites with different ratios were prepared. And the composites were recorded as MCN@NiCo₂O₄-0.5, MCN@NiCo₂O₄-1 and MCN@NiCo₂O₄-2 in following experiment, respectively.

For comparison, the pure NiCo₂O₄ was synthesized by the procedure similar to the above method without adding MCN.

1.3.3 Preparation of MCN@NiCo₂O₄ coated fiber

Stainless steel wires with a diameter of 0.1 mm were employed as support for preparation MCN@NiCo₂O₄ coated fiber. All stainless steel wires have pre-treated by an immersion into a nitric acid: hydrochloric acid mixture solution (1:3, v/v) for 5 min to ensure an enough porosity on the wire surface. After cleaning, the treated stainless steel wires were immersed into sol-SiO₂ for 1 min, and then MCN@NiCo₂O₄ powder was stuck to stainless steel wires, dried and repeated 10 times. Finally, the MCN@NiCo₂O₄ coated fiber was heated in an vacuum oven at 80 °C for 12 h. Prior to use, all the fibers were assembled into a 5 μL microsyringe to make up a SPME device and exposed at 290 °C 1 h in GC injector port for activation to avoid any contamination.

1.4 Sample preparation

The blood samples were extracted from a volunteer by venipuncture in sterilized vacutainer blood tubes. Human blood serum was obtained by whole blood sample

centrifugation at 6000 rpm for 10 min and stored at -20 °C prior to use.

1.5 HS-SPME procedures

Herein, headspace-SPME (HS-SPME) was selected to decrease the damage of fiber coating and eliminate the interferences from complex matrices. For HS-SPME mode, 1.0 mL of human serum sample diluted with ultrapure water to 10.0 mL was placed into 20 mL glass vial and immediately sealed with PTFE-coated septum. A thermostatic water bath was chosen to control the extraction temperature, a Teflon-coated stir bar with magnetic stirring was used to agitate the solution and a certain quantity of NaCl was to give salting out effect. During the extraction, the fiber was carefully introduced directly into the headspace above the solution for a certain time. After extraction, the fiber was immediately inserted into GC injector port for thermal desorption and the fiber was conditioned at 290 °C for another 15 min before next extraction.

1.6 Determination of enrichment factors

The adsorption affinity between the MCN@NiCo₂O₄ fiber coating and the tested analytes were investigated in terms of the enrichment factor (EF), which was defined as the ratio of the analyte concentration after extraction and the original concentration. The following equation was used to calculate the EF parameter:

$$EF=C_f/C_s$$

Where C_f is the concentration of analyte after extraction and C_s is the concentration of analyte originally existed in the sample solution. The direct injection of 1 μ L of standard solution from 0.5-500 μ g·mL⁻¹ of analytes was performed to obtain the chromatographic peak areas.

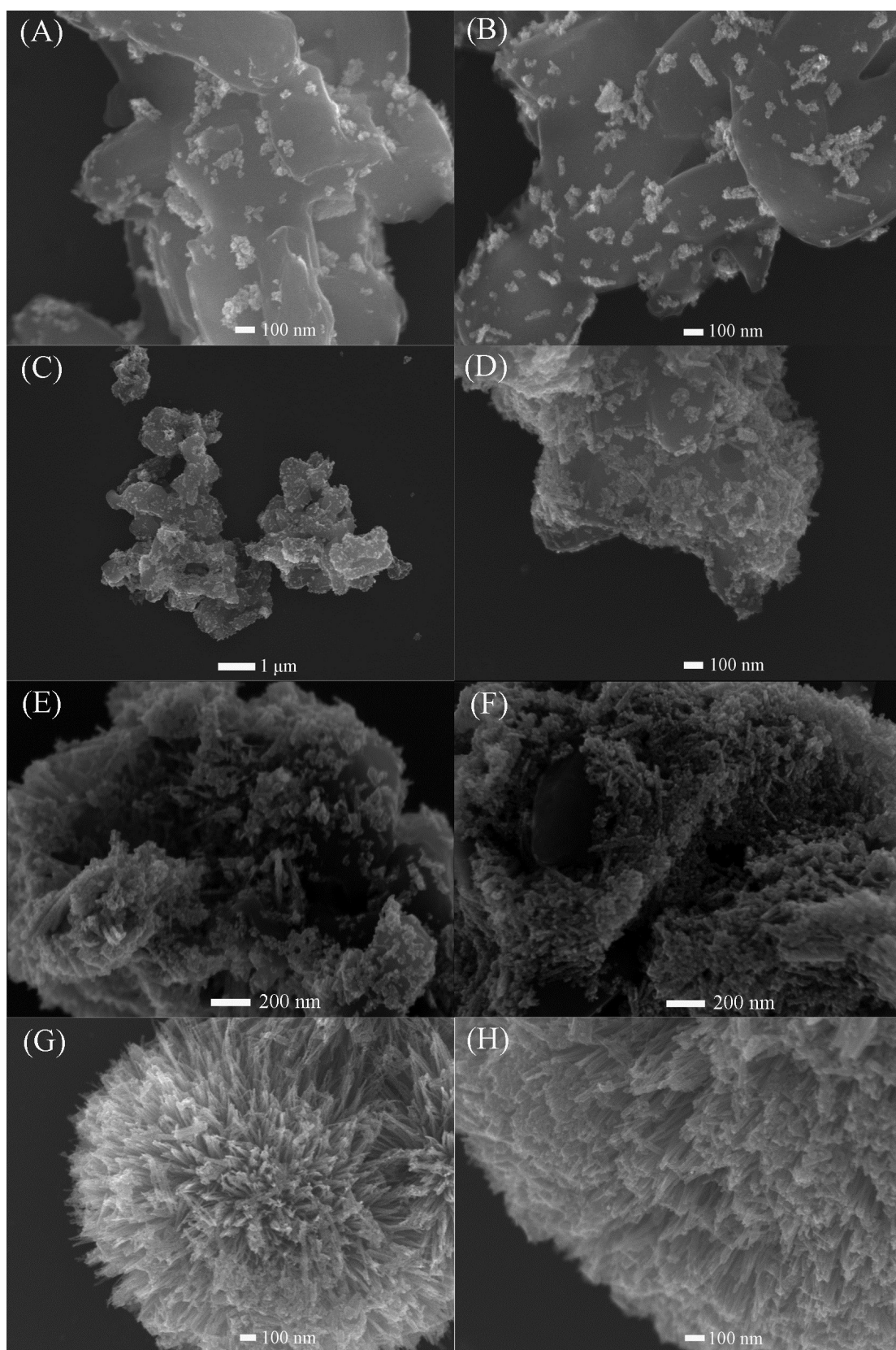


Fig. S1 SEM images of the MCN@NiCo₂O_{4-0.5} (A, B), MCN@NiCo₂O₄₋₁ (C, D), MCN@NiCo₂O₄₋₂ (E, F) and pure NiCo₂O₄ (G, H).

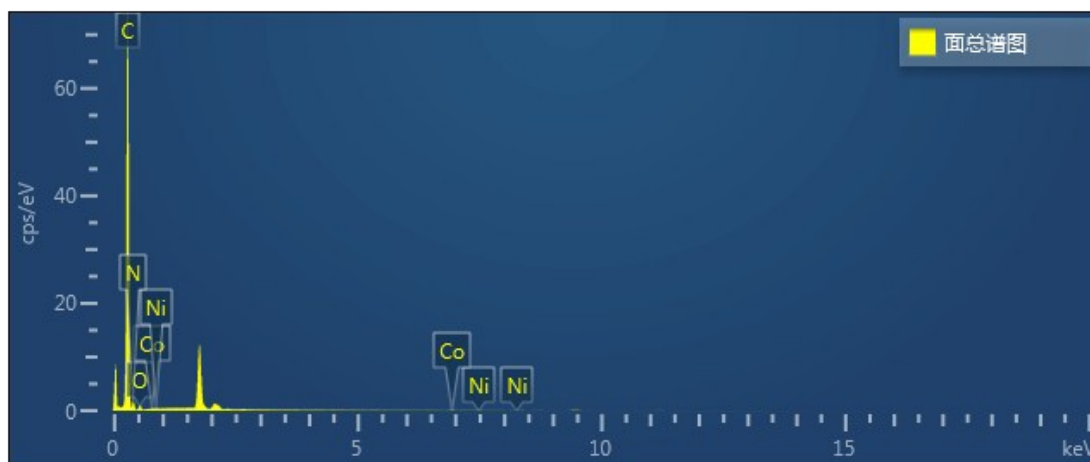


Fig. S2 The element type analysis of MCN@NiCo₂O₄ on energy dispersive spectrometer (EDS)

Table S1 The content analysis of MCN@NiCo₂O₄ on energy dispersive spectrometer (EDS)

element	weight percent(%)	atomic percent(%)
C	39.89	58.55
O	24.02	26.47
Co	21.02	6.29
Ni	10.72	3.22
N	4.35	5.47

2 Optimization of HS-SPME procedures

2.2.1 Extraction temperature

As one of the significant parameters effects on the headspace extraction efficiency, the extraction temperature was investigated from 30 to 80 °C. As shown in Fig. S3A, the peak areas of all analytes increased rapidly from 30 to 60 °C and then reached the maximum plateau. Generally, increasing the extraction temperature can improve the diffusion of analytes from bulk water phase to headspace and accordingly facilitate the coating adsorption. Nevertheless, most surface adsorption process is an exothermic process, excessive high temperature may decrease the extraction efficiency. Therefore, the extraction temperature of 60 °C was chosen for the following experiments.

2.2.2 Extraction time

SPME is an equilibrium-based extraction procedure, and sufficient time is need to transfer of analytes from sample solution to the MCN@NiCo₂O₄ coated fiber. In this experiments, the effect of extraction time was investigated from 10 to 60 min. The results shown in Fig. S3B presented that the peak areas of all analytes continue to increase until reached equilibrium at 30 min and then slightly decreased. Considering both sides of getting maximum extraction efficiency and saving time, 30 min was selected as the most suitable extraction time.

2.2.3. Desorption temperature

Desorption temperature is another key parameter that effect on the extraction efficiency for SPME. As we know, increasing the desorption temperature can completely release analytes from the fiber coating to provide a satisfactory sensitivity while inevitably shorten lifetime of the fiber. Therefore, the desorption temperature was systematically investigated in the range of 240 to 300 °C (Fig. S3C). It is obviously observed that the response signal of the PCB-14, PCB-12, PHE, ANT and PYR showed an upward trend from 240 to 290 °C. When the desorption temperature

higher than 290 °C, the response signals of the NAP, ANE, PCB-3 and FLU have slightly decrease. Consequently, the desorption temperature was set at 290 °C.

2.2.4. Desorption time

The desorption time is another important desorption conditions. A suitable desorption time can not only insure the analytes fully released from the fiber but also avoid the crossover contamination in following experiments. Otherwise, the long-term desorption in GC injector port may cause the fiber to be broken due to the incessant high temperature. Therefore, the desorption time was investigated from 0.5-3.0 min while the desorption temperature was set as 290 °C. Result shown in Fig. S3D revealed that the desorption efficiency was enhanced with increasing the desorption time from 0.5 to 2.5 min and subsequent kept almost constant. Hence, 2.5 min was sufficient for the analytes to desorb from the MCN@NiCo₂O₄ coated fiber at 290 °C.

2.2.5. Agitation speed

The agitation speed is another factor influencing the diffusion of analytes into the headspace which was also studied in this experiment. In general, effective agitation can increase transfer of analytes from sample solution to the headspace and shorten the equilibrium time. However, an excessive stirring speed may reduce the extraction efficiency due to the formation of bubbles inside the solution and the volatile analytes assumed around the bottle cap. The agitation speed was investigated from 0 to 1200 rpm in Fig. S3E, the peak areas of the analytes increased slightly as increasing the agitation speed from 0 to 1000 rpm and up to the maximum at 1000 rpm. As a consequence, the optimal agitation speed was considered to be 1000 rpm.

2.2.6 Salt concentration

The addition of salt can increase the ionic strength of solution, and cause salting-out effect so that affect the headspace extraction efficiency. The extent of this influences depended on both sides of chemical structure and salt concentration. Therefore, NaCl was selected to adjust ionic strength and different concentration from 0 to 30% (w/v) was evaluated in this study. As seen from Fig. S3F, the peak areas of

six PAHs increased slightly with adding NaCl. However, the extraction efficiency of the three PCBs increased with increasing NaCl concentration from 0% to 10% (w/v) and then appear decrease or rise-fall tendency with the further increasing NaCl concentration from 10% to 30% (w/v). This phenomenon can be explained by two processes that occurred simultaneously in the extraction process. On the one hand, from the thermodynamic point of view, the addition of NaCl salt due to the salting-out effect, which reduced the solubility of the target PCBs in the aqueous phase and promote the diffusion of analytes to the fiber coating so that leading to an increase in the amount of analytes extracted by MCN@NiCo₂O₄ coated fiber. On the other hand, from a kinetic point of view, addition of NaCl salt can enhance the viscosity and density of the aqueous phase which is unfavorable for the extraction efficiency.² Thus, NaCl concentration of 10% (w/v) in the sample solution was employed for further investigation.

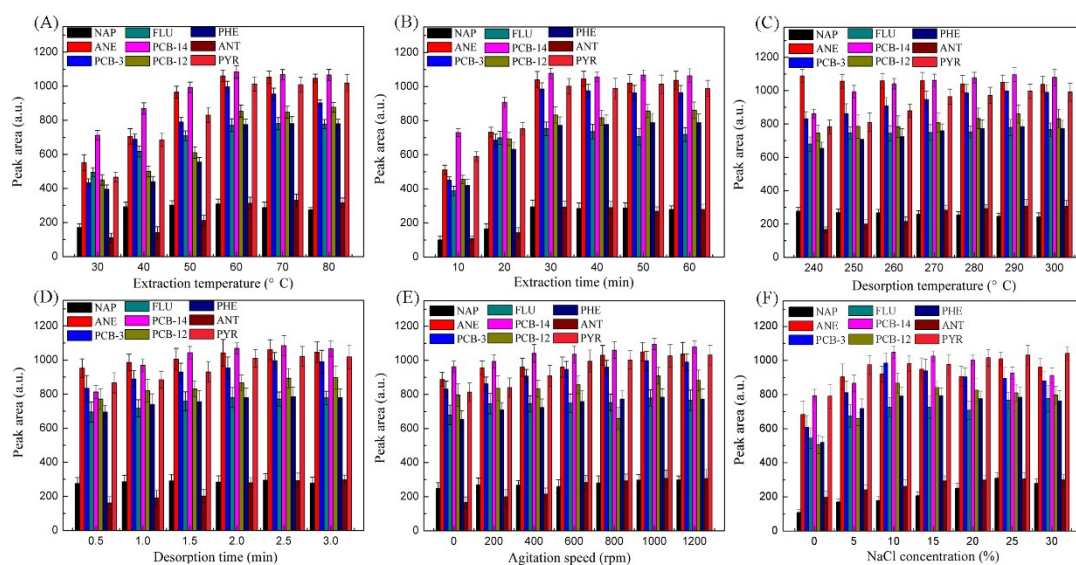


Fig. S3 Effect of the experimental conditions on extraction efficiency of MCN@NiCo₂O₄ coated fiber for 100 ng·mL⁻¹ PCBs and PAHs. (A) Extraction temperature; (B) Extraction time; (C) Desorption temperature; (D) Desorption time; (E) Agitation speed; (F) NaCl concentration. Error bar shows the standard deviation for triplicate determinations (n=3).

3. Analytical performance of the MCN@NiCo₂O₄ coated fiber

3.1 Comparison of the different ratios MCN@NiCo₂O₄ coated fibers with pure NiCo₂O₄ and MCN coated fiber

The extraction performance of different ratios MCN@NiCo₂O₄ coated fibers

were compared with the pure NiCo₂O₄ and MCN coated fiber, respectively. As the results shown in Fig. S4, the MCN@NiCo₂O₄ coated fiber provided the higher peak areas for the target analytes than the pure NiCo₂O₄ and MCN coated fiber at the same conditions, demonstrated that the prepared MCN@NiCo₂O₄ nanocomposite was a favorable coating for extraction PCBs and PAHs. Compared the three different ratios MCN@NiCo₂O₄ coated fibers, it is obviously observed that the extraction efficiency increased as the ratio of MCN increasing. The superior extraction performance of MCN@NiCo₂O₄ coating can be attributed to its advantageous porosity, meanwhile, the synergistic effects including π - π interaction hydrophobic interaction and hydrogen bonding interaction between the coating and target analytes.

Lifetime is another key factor to evaluate the performance of the fiber coating. The lifetimes of the fibers were investigated by subjecting a standard solution of target analytes at 100 ng·mL⁻¹ to several adsorption/desorption cycles. From Fig. S3, it can be seen that the extraction performance of MCN had an obvious decline after being extracted 5 times. When a handful of NiCo₂O₄ incorporated with MCN, the extraction performance has been greatly improved while the life time of the MCN@NiCo₂O₄-0.5 coated fiber was too short (remarkable decreased after 2 extraction cycles). While the MCN@NiCo₂O₄-1 coated fiber was still acceptable after 150 times extraction after moderate incorporation of NiCo₂O₄, indicating an excellent durability of MCN@NiCo₂O₄-1 coated fiber. When there are relatively large numbers of NiCo₂O₄ incorporation, the MCN@NiCo₂O₄-2 coated fiber showed a long life time just like pure NiCo₂O₄, but the extraction performance was not well. It can be attributed to that a large number of NiCo₂O₄ grew on the outside of MCN and occupied a certain adsorption sites.

Therefore, considering both extraction efficiency and life time of the fiber, MCN@NiCo₂O₄-1 has been selected in this study.

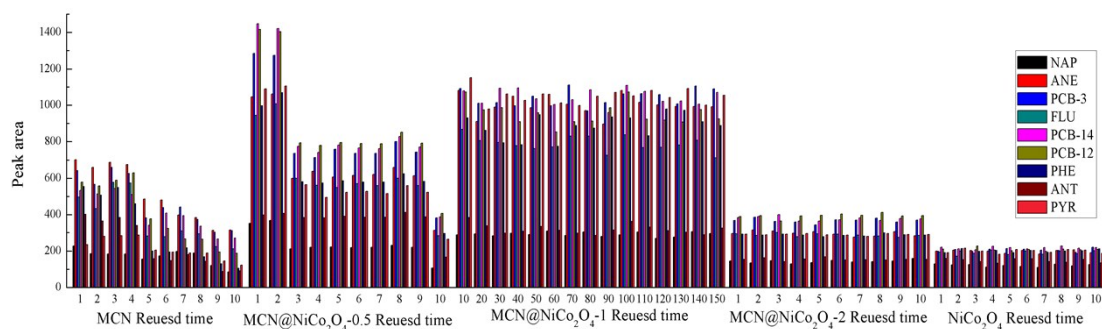
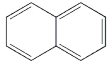
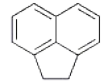
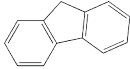
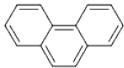
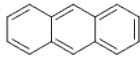
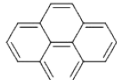
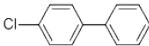
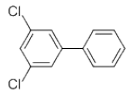
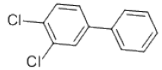



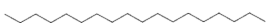






Fig. S4 Comparison the extraction performance and lifetime of the different ratios MCN@NiCo₂O₄ coated fibers with pure NiCo₂O₄ and MCN coated fiber.

3.2 The features and further applications

MCN which has the larger surface area, special porosity, in-built N-rich functional groups and electronic delocalization properties endow the MCN with complex extraction mechanism, involving π - π conjugation, hydrogen bond interaction, electrostatic interaction and hydrophobic effect^{3,4}. The NiCo₂O₄ metal oxides whose structure Ni occupies the octahedral sites and Co is fixed in the octahedral and tetrahedral sites have a large nature abundance ability. NiCo₂O₄ is also a promising transition metal oxides for pseudocapacitors owing to its intriguing electronic conductivity, low diffusion resistance to protons/cations, and easy electrolyte penetration⁵⁻⁸. The MCN@NiCo₂O₄ composite remain both advantages of MCN and NiCo₂O₄, is looking forward to further exploit for other applications in photocatalysis, supercapacitors, fuel cells, gas storage, electrogenerated chemiluminescence, sensing and bioimaging.

Table S2 Physical-chemical properties of different analytes and the enrichment factors (EFs) for the analytes on the MCN@NiCo₂O₄ coated fiber (n=3)

Analyte	Structure	Molecular weight	$\log K_{ow}^a$	EFs
NAP		128.171	3.30	1235
ANE		154.208	3.92	2187
FLU		166.219	4.18	1722
PHE		178.229	4.46	2420
ANT		178.229	4.45	1590
PYR		202.251	4.88	2674
PCB-3		188.653	4.61	3765
PCB-14		223.098	5.41	4094
PCB-12		223.098	5.29	3924
Undecane		156.308	5.74	93
Dodecane		170.335	6.10	128
Tetradecane		198.388	7.20	136
Octadecane		254.494	9.18	171
Undecanol		172.308	4.28	367
Dodecanol		186.334	5.13	424
Tetradecaneol		214.387	6.03	472
Octadecanol		270.494	7.72	529

^a $\log K_{ow}$: n-octanol/water partition coefficients, indicator for hydrophobicity. Data taken from RSC publishing Home: <http://www.chemspider.com/>

Table S3 The Linearity, LOQs, LODs and precision parameters of the method 3.30 for the analysis of PCBs and PAHs.

Analytes	Linearity			LOQs (pg·mL ⁻¹)	LODs (pg·mL ⁻¹)	Precision (RSDs,%)		
	Range (ng·mL ⁻¹)	Linear equation	r			Intraday (n=5)	Interday (n=5)	Fiber to fiber (n=3)
NAP	0.010-0.50	$y = 33.921x + 0.2744$	0.9952	10.0	3.1	2.83	5.26	7.10
	0.50-100.0	$y = 3.14x + 12.116$	0.9996					
ANE	0.005-0.50	$y = 36.069x + 0.7029$	0.9944	5.0	2.7	6.83	7.25	11.74
	0.50-100.0	$y = 5.8599x + 6.2227$	0.9987					
PCB-3	0.002-0.50	$y = 36.069x + 0.7029$	0.9956	2.0	0.9	7.21	7.61	9.90
	0.50-100.0	$y = 9.9539x + 56.244$	0.9993					
FLU	0.010-0.50	$y = 9.1091x + 0.3701$	0.9956	10.0	2.3	6.80	8.42	6.28
	0.50-100.0	$y = 2.9832x + 5.4918$	0.9989					
PCB-14	0.002-0.50	$y = 83.584x + 1.3763$	0.9959	2.0	1.2	5.78	6.30	4.62
	0.50-100.0	$y = 9.8447x + 39.78$	0.9993					
PCB-12	0.002-0.50	$y = 86.972x + 0.6814$	0.9997	2.0	1.2	7.47	9.62	7.03
	0.50-100.0	$y = 7.9901x + 46.815$	0.9989					
PHE	0.005-0.50	$y = 71.901x + 1.1211$	0.9971	5.0	1.6	5.60	8.74	11.84
	0.50-100.0	$y = 7.369x + 32.973$	0.9991					
ANT	0.010-00.50	$y = 31.793x + 0.1017$	0.9975	10.0	3.3	6.86	9.09	13.12
	0.50-100.0	$y = 3.0364x + 25.184$	0.9984					
PYR	0.002-0.50	$y = 98.121x + 0.5771$	0.9998	2.0	1.2	5.29	9.02	8.78
	0.50-100.0	$y = 10.594x + 13.081$	0.9998					

Table S4 Comparison of the different fibers for the SPME of PCBs and PAHs.

Analytes	Sorbents	Sample	LODs (pg·mL ⁻¹)	Analytical method	Lifetime (times)	Refs.
PAHs	3D-IL-Fe ₃ O ₄ -GO	Human blood	20.0-50.0	PT-SPE-GC-FID	-	9
PAHs	Sol-gel CNF-PDMS	Water	5.0-20.0	SPME-GC-FID	≥180	10
PAHs	AgNPs	Water	600-14000	SPME-GC-FID	≥150	11
PAHs	IL-hybridized sol-gel	Cigarette smoke Cigarette ash	15.0-30.0	SPME-GC-FID	≥120	12
PAHs	PEDOT@AuNPs	Water, soil	2.5-25.0	SPME-GC-FID	≥160	1
PAHs	Graphene	Water	1.0-20.0	SPE-GC-FID	- ^a	13
PAHs	MCN@NiCo ₂ O ₄	Human serum	1.2-3.3	SPME-GC-FID	≥150	This work
PCBs	PDMS	Human serum	70.0-1790	SPME-GC/MS	-	14
PCBs	PDMS	Human serum	1.0-12.0	SPME-GC-ECD	-	15
PCBs	-	Human serum	3.0-47.0	SB-μ-SPE-GC/MS	-	16
PCBs	C18	Human serum	8.0-44.0	SPE-GC/HRMS	-	17
PCBs	Poly-IL	Water	0.9-5.8	SPME-GC-ECD	≥250	18
PCBs	MIL-53(Fe)	Soil	50.0-90.0	SPME-GC-MS	≥50	19
PCBs	MCN@NiCo ₂ O ₄	Human serum	0.9-1.2	SPME-GC-FID	≥150	This work

^a Not mentioned.

Table S5 The recoveries of the developed method for analysis of target analytes in serum sample.

Analytes	Add (ng·mL ⁻¹)	Found (ng·mL ⁻¹)	Recovery (%)	RSDs (n=3, %)
NAP	0	N.D. ^a	-	-
	0.1	0.11	98.3-119.0	10.1
	5.0	4.38	82.7-93.5	6.3
	10.0	11.09	104.1-115.6	5.4
ANE	0	0.66	-	-
	0.1	0.09	80.0-96.6	9.4
	5.0	5.24	99.9-110.5	5.1
	10.0	9.79	93.0-106.4	7.6
PCB-3	0	0.70	-	-
	0.1	0.11	104.5-118.0	6.1
	5.0	4.22	75.1-90.9	9.8
	10.0	10.43	95.8-111.5	7.6
FLU	0	N.D. ^a	-	-
	0.1	0.11	105.8-119.8	6.3
	5.0	4.70	86.5-99.3	7.0
	10.0	8.05	76.8-83.2	4.1
PCB-14	0	0.78	-	-
	0.1	0.12	110.0-121.2	4.8
	5.0	5.35	93.7-115.4	10.9
	10.0	7.96	76.2-85.1	6.1
PCB-12	0	0.45	-	-
	0.1	0.10	95.6-109.4	6.8
	5.0	4.05	74.8-91.1	10.8
	10.0	7.77	72.4-85.1	7.8
PHE	0	N.D. ^a	-	-
	0.1	0.12	110.2-119.5	4.1
	5.0	4.47	79.6-95.3	9.6
	10.0	7.87	73.7-87.4	9.7
ANT	0	N.D. ^a	-	-
	0.1	0.10	88.0-110.0	11.1
	5.0	4.46	79.8-98.2	10.3
	10.0	10.39	97.5-111.7	6.9
PYR	0	0.09	-	-
	0.1	0.11	100.1-113.4	6.2
	5.0	5.00	90.7-107.3	8.5
	10.0	7.52	72.5-79.3	4.8

^aNot

detected.

Reference

1. L. Yang, J. Zhang, F. Zhao and B. Zeng, *J. Chromatogr. A*, 2016, **1471**, 80.
2. F. Lv, N. Gan, Y. Cao, Y. Zhou, R. Zuo and Y. Dong, *J. Chromatogr. A*, 2017, **1525**, 42.
3. J. Zhang, W. Li, W. Zhu, Y. Yang, P. Qin, Q. Zhou and M. Lu, *Microchim. Acta*, 2019, **2**, 1–9.
4. M. Ghaemmaghami, Y. Yamini, H. Amanzadeh and B. H. Monjezi, *Chem. Commun.*, 2018, **54**, 507–510.
5. Y. Wei, S. Chen, D. Su and B. Sun, *J. Mater. Chem. A*, 2014, **2**, 8103–8109.
6. G. Zhang, X. Wen and D. Lou, *Adv. Mater.*, 2013, **25**, 976–979.
7. D. U. Lee, B. J. Kim and Z. Chen, *J. Mater. Chem. A*, 2013, **1**, 4754–4762.
8. N. Iqbal, X. Wang, A. Ahmed, J. Yu and B. Ding, *J. Colloid. Interface. Sci.*, 2016, **476**, 87–93.
9. Y. Zhang, Y. Zhao, W. Chen, H. Cheng, X. Zeng and Y. Zhu, *J. Chromatogr. A*, 2018, **1552**, 1.
10. Amiri and F. Ghaemi, *Microchim. Acta*, 2016, **183**, 1917.
11. A. Gutiérrez-serpa, P. I. Napolitano-tabares, V. Pino and F. Jiménez-moreno, *Microchim. Acta*, 2018, **185**, 341.
12. Y. Tian, J. Feng, X. Wang, C. Luo and M. Sun, *J. Chromatogr. A*, 2019, **1583**, 48.
13. A. Amiri and F. Ghaemi, *Anal. Chim. Acta*, 2017, **994**, 29.
14. R. Flores-ramírez, M. D. Ortiz-pérez, L. Batres-esquivel and C. G. Castillo, *Talanta*, 2014, **123**, 169.
15. A. Etxandia, E. Mill, L. Raul and F. Go, *J. Chromatogr. B*, 2007, **846**, 298.
16. M. Sajid and C. Basheer, *J. Chromatogr. A*, 2016, **1455**, 37.
17. J. Wittsiepe, M. Nestola, M. Kohne, P. Zinn and M. Wilhelm, *J. Chromatogr. B*, 2014, **945–946**, 217.
18. J. Li, F. Wang, J. Wu and G. Zhao, *Microchim. Acta*, 2017, **184**, 2621.
19. F. Lv, N. Gan, J. Huang, F. Hu, Y. Cao and Y. Zhou, *Microchim. Acta*, 2017, **184**, 2561.